Institute of Space and Aeronautical Science, University of Tokyo
Report No. 434, January 1969

A Numerical Study of Particle Acceleration in the Magnetosphere

By

Tsutomu TAMAO and Osamu ASHIHARA

Summary: In order to obtain the quantitative result for wave-particle interaction within the complicated magnetospheric configuration, the Fermi acceleration of energetic electrons trapped within the dipole magnetic field due to the interaction with a large-amplitude hydromagnetic pulse is numerically analysed, under the condition of the magnetic moment conservation. Associated with the geomagnetic sudden commencement, if this pulse propagates from the equator to high latitudes along the particular field line multiple head-on collisions of the particle with the moving pulse yield the net acceleration and secular lowering of the mirror point, until the mirror point is overtaken by the pulse. Assuming a model distribution of the plasma density and Poynting flux conservation of the pulse during its propagation, the motion of an interacting electron is determined in detail for various initial equatorial pitch angle. It is shown that the acceleration by this process is most effective for trapped particles near the equator. From results of the present numerical study, however, we cannot expect the appreciable particle precipitation associated with the geomagnetic ssc by only consideration of the Fermi process, and other more intense acceleration mechanism will be necessary in the real magnetosphere.

1. INTRODUCTION

There have been many observational indications of the particle acceleration and precipitation into the ionosphere in high latitudes associated with several geomagnetic disturbances, for examples, the sudden commencement of a storm, geomagnetic pulsations, and polar substorm [*1*]. In particular, the sudden intense precipitation of energetic particles at the phase of auroral break-up in the geomagnetic bay will be the most essential process for the polar disturbances, and its unsolved mechanism may be strongly connected with nonlinear wave-particle interactions in plasmas.

Generally speaking, acceleration of charged particles can be estimated when a spectrum of the associated disturbances of electric and magnetic fields is given, irrespective of the type of acceleration process, that is, the direct or stochastic accelerations. If the mean energy of accelerating particles is small compared with that of the ambient plasma, the result of acceleration does not modify the original accelerating field, so that the picture of a single particle acceleration can be applied. A representative of this case is the Fermi acceleration of cosmic-ray particles [*2*]. On the other hand, if the energy density of interacting particles is the same order of magnitude with that of the accelerating field or the ambient plasma, the feedback

effect of accelerated particles will appreciably modify the spectrum of field. Hence the problem essentially becomes the collective interaction. For weak interactions, the quasilinear theory of stochastic acceleration is an appropriate method for describing these collective nonlinear interactions [*3*].

Our present knowledge concerning electric and magnetic disturbances within the magnetosphere is far from satisfactory to obtain the accurate estimation of possible particle acceleration. However, some basic process to be important for the precipitation have thus far been studied by several workers. Cyclotron-resonance and bounce-resonance interactions yield the velocity space diffusion to decrease the pitch angle of energetic particles and lead to the particle loss from the trapped region [*4, 5*]. Quasilinear interaction of these processes would result some equipartition between the available free energy of trapped particles and the associated unstable waves, and then determine the threshold of trapped particles. It seems that some observations require the more rapid and intense interaction process. Acceleration by the electric field parallel to the ambient magnetic field [*6, 7, 8*], or enhancement of the loss-cone instability [*9*] due to the adiabatic compression may be effective for such situation.

In addition, from the simultaneous observations of the geomagnetic field, cosmic noise absorption, and X-ray burst, we have the sudden commencement precipitation of energetic electrons with the time scale of several hundreds second [*1, 10*]. It would have been believed that an association of the large-scale hydromagnetic wave pulse propagating along field lines in the magnetosphere with energetic electrons can cause such precipitation event [*11*]. If hydromagnetic disturbances are considered as the accelerating agency, for which the first invariant of the interacting particle is conserved, we have two fundamental processes. One of them is the transit-time acceleration of the bouncing particles by the standing hydromagnetic oscillations with nonuniform amplitude. Theoretical studies of this process were quantitatively performed and the resulting effect for the life time of trapped electrons in the outer radiation belt was discussed [*5, 12*]. The other is the Fermi acceleration resulting from multiple reflections of the interacting particle by the propagating large-amplitude pulse. A bouncing wave packet with a centered frequency will have some combined effects to the particle acceleration.

In the present paper, as a first step to the quantitative study of wave-particle interaction within the complicated magnetospheric situation, the problem of the Fermi acceleration of energetic electrons trapped in the geomagnetic dipole field by the large-amplitude compressive pulse propagating along the particular field line will be numerically analysed.

2. Basic Equations for the Interaction

Let us consider the motion of a charged particle along a line of the geomagnetic dipole field. In addition to the ambient magnetic field, if we superpose the hydromagnetic perturbation for which the magnetic moment of the particle is conserved, the non-relativistic equation of the parallel motion of the particle is given by

$$mdu/dt = q\delta E_{\parallel} - \mu\partial(B_0 + \delta B)/\partial s\,, \qquad (1)$$

where u is the parallel component of the particle velocity, $B_0(s)$ the intensity of the dipole magnetic field, $\delta E_{\parallel}$ and δB are the parallel electric field and the intensity of the perturbation magnetic field, respectively, and s is a distance along the field line. $\mu = w_{\perp}/B = mv^2 \sin^2\alpha/2B$ is the magnetic moment of the particle whose total velocity is v and pitch angle α, and B is the total magnetic intensity at the instantaneous position of a guiding center of the particle. On the right hand side of (1), the first term gives the Landau acceleration while the last term yields the Fermi or transit-time acceleration. Based on (1), Barnes discussed the stochastic heating of plasma for the case of a uniform ambient magnetic field [*13*].

On the other hand, the parallel component of electric field of hydromagnetic perturbations is related to the associated magnetic perturbation, and approximately given by [*14*]

$$\delta E_{\parallel} = (\beta_{\perp}/2)(\omega/\Omega_i)(\omega/k_{\parallel})\delta B_{\parallel}\,, \qquad (2)$$

where $\beta_{\perp} = 8\pi nKT_{\perp}/B_0^2$ is a ratio of gas pressure of the ambient plasma to magnetic pressure, Ω_i the ion Larmor frequency, and ω and k are the angular frequency and wave number in the parallel direction of the hydromagnetic perturbation. Since $\delta B = \delta B_{\parallel}$ in the first order approximation, substitution of (2) into (1) leads

$$|q\delta E_{\parallel} 1/1(\mu/q)\partial\delta B_{\parallel}/\partial s| \sim KT_{\perp}/w_{\perp}\,. \qquad (3)$$

Consequently, the effect of the parallel electric field can be neglected comparing with that of the magnetic force, if the kinetic energy of the accelerating particle is much larger than the mean temperature of the ambient plasma, i.e. $KT_{\perp}/w_{\perp} \ll 1$. It is, however, noted that a possibility of the particle acceleration due to the parallel electric field of some electrostatic mode perturbations cannot be eliminated.

Next, let us consider a form of the large-scale magnetic pulse propagating from the equator to lower altitudes along the particular field line. If we assume the conservation of the Poynting flux of the hydromagnetic pulse in the direction parallel to the ambient field line, it is easily shown that the amplitude of the associated magnetic perturbation is proportional to the fourth root of the local plasma density. Thus, we take the following forms of the magnetic perturbation

$$\delta B_{\parallel}(s, t) = \delta B_E[\rho(s)/\rho_E]^{1/4} \exp\left[-a^2(t - |\tau|)^2\right], \qquad (4)$$

for $t - |\tau| < 0$, where $\tau(s)$ is defined by

$$\tau(s) = \int_0^s ds'/V_A(s')\,, \qquad (5)$$

and

$$\delta B_{\parallel}(s, t) = \delta B_E[\rho(s)/\rho_E]^{1/4} \quad \text{for} \quad t - |\tau| \geq 0\,. \qquad (6)$$

Here δB_E is the perturbed magnetic intensity at the equator, ρ_E the equatorial plasma density, $V_A(s)=B_0(s)[4\pi\rho(s)]^{-1/2}$ the local Alfvén speed at the instantaneous position of the interacting particle and a is a constant.

To determine the trajectory of the interacting particle, the following equation is further required

$$ds/dt=u(s, t)\,. \tag{7}$$

3. A Simple Fermi Acceleration

Before considering the complicated situation, in this section we give some preliminary analyses for the Fermi acceleration of a charged particle by the uniformly moving magnetic wall under the uniform stationary condition. As this moving wall, we assume the expression of (4) with the constant amplitude δB_0. The equation of motion of the particle becomes then

$$du/dt=-(\mu/m)\delta B_0(2a^2/V_A)(t-|\tau|)e^{-a^2(t-|\tau|)^2}\,, \tag{8}$$

where V_A is a constant Alfvén speed. For the initial conditions, $t=0$; $s=s_0$ and $u=-u_0<0$, integration of the above equation leads as

$$(u/u_0)^2-2\alpha(u/u_0)-[1+2\alpha(1-C)]=0\,, \tag{9}$$

where C is defined by

$$C=(\beta\varepsilon/\alpha)[e^{-a^2(t-s/V_A)^2}-e^{-a^2(s_0/V_A)^2}]\,,$$

and $\alpha=V_A/u_0$, $\beta=w_\perp(t=0)/w_\parallel(t=0)$, $\varepsilon=\delta B_0/B_0$.
From (9), we have

$$u(t)/u_0=\pm\{(1+\alpha)[1-2\alpha(1+\alpha)^{-2}C]^{1/2}\pm\alpha\}\,, \tag{10}$$

where we take $-$ sign before reflection and $+$ sign for the reflected particle.

If we suppose the asymptotic time limit after reflection of the particle, C tends to $C_\infty=-(\beta\varepsilon/\alpha)e^{-a^2(s_0/V_A)^2}$, consequently

$$u_\infty/u_0=\alpha+(1+\alpha)[1+2\alpha|C_\infty|(1+\alpha)^{-2}]^{1/2}\,. \tag{11}$$

Except the correction term in the square root due to the finite width of the moving wall, this result coincides with that of a case of the discontinuous step function, for which the velocity increase of the particle after a single reflection is $\delta u=2V_A$.

Next, we consider the condition of the particle reflection at the wall for the given initial parameters. At the reflection point, we have

$$(1+\alpha)[1-2\alpha(1+\alpha)^{-2}C_{\rm ref}]^{1/2}-\alpha=0\,,$$

where $C_{\rm ref}$ is the value of C at the reflection. Therefore, in order to have the reflection, the necessary condition becomes

$$C\geq C_{\rm ref}=[(1+\alpha)^2/2\alpha][1-\alpha^2(1+\alpha)^{-2}]\,.$$

While, from the definition of C we have $C<\beta\varepsilon/\alpha$. Thus, we obtain the following condition for the reflection

$$(\alpha^2+\varepsilon\beta)(1+\alpha)^{-2}\equiv\frac{(V_A/u_0)^2+(\delta B_0/B_0)(w_\perp/w_\parallel)}{[1+V_A/u_0]^2}>1\,. \tag{12}$$

Since $V_A/u_0\ll 1$ for energetic particles, this condition requires the large amplitude magnetic perturbation with $\delta B_0\sim B_0$.

Lastly, let us extend the result of the above simple Fermi process to the inhomogeneous mirror configuration. We suppose a charged particle whose kinetic energy and pitch angle at the point of the minimum magnetic intensity B_0 are w_0 and α_0, respectively, and the magnetic intensity at the initial mirror point is B_m. After a head-on collision with the magnetic wall propagating to the initial mirror point, the reflected particle is accelerated by δw_0 and its pitch angle changes by $\delta\alpha_0$, so that the new mirror point moves to the point corresponding to $B_m+\delta B_m$. For this situation, conservation of the particle magnetic moment leads

$$\frac{w_0\sin^2\alpha_0}{B_0}=\frac{w_0}{B_m}=\frac{w_0+\delta w_0}{B_m+\delta B_m}=\frac{(w_0+\delta w_0)\sin^2(\alpha_0+\delta\alpha_0)}{B_0}$$

From these, we have

$$\delta B_m/B_m=\delta w_0/w_0\,,$$

and

$$(1+\delta w_0/w_0)^{1/2}\sin(\alpha_0+\delta\alpha_0)=\sin\alpha_0\,.$$

Using the acceleration rate through a single collision, $\delta w_0\sim mu_0V_A$ and $\delta\alpha_0\ll 1$, the above two equations yield

$$\delta B_m\sim 2(V_A/u_0)B_m\,,$$

and

$$\delta\alpha_0\sim-\tan\alpha_0[1-(1+\delta w_0/w_0)^{-1/2}]\sim-(\delta w_0/2w_0)\tan\alpha_0<0\,.$$

From these relations we can estimate the order of magnitude of the lowering of the mirror point and the decrease of pitch angle. If the initial distance between the particle mirror point and the wave front is l, the total acceleration by multiple reflections during the time before the overtaking of the mirror point by the wave front is of about $\delta w/w_0\sim 4(V_A/u_0)(l/V_A)/(2l/u_0)\sim 2$.

4. Models for the Numerical Calculation

Particle motion in the stationary dipole field

In this section, first we give shortly the characteristics of a single particle motion under the dipole magnetic field, which become necessary for the numerical analysis

in the next section as the initial conditions. Preliminary numerical calculations in this section are also useful to check the method for the more complicated situation.

In spherical coordinates (r, θ, φ), the intensity of magnetic field on the field line which cuts the equatorial plane at the radial distance r_E is given by

$$B_0(r_E, \theta)=(M/r_E^3 \sin^6\theta)(1+3\cos^2\theta)^{1/2}, \tag{13}$$

where M is a magnetic moment of the dipole. Now let us define s as the distance along the field line from the equatorial plane such that s is positive in the northern hemisphere and negative in the southern hemisphere. After this definition, we have $ds=-\sin\theta(1+3\cos^2\theta)^{1/2}d\theta$. Then,

$$\frac{dB_0}{ds}=\frac{3B_E\cos\theta}{r_E\sin^8\theta}\left(2+\frac{\sin^2\theta}{1+3\cos^2\theta}\right), \tag{14}$$

where B_E is the equatorial value of B_0.

On the other hand, the bouncing period of the particle, whose equatorial pitch angle is α_E and mirror points are $\pm\theta_m$, is given as

$$T_b=4(r_E/u_0)\int_{\theta_m}^{\pi/2}\frac{\sin\theta(1+3\cos^2\theta)^{1/2}}{[1-(B_0(s)/B_E)\sin^2\alpha_E]^{1/2}}d\theta, \tag{15}$$

where $u_0=(2w_0/m)^{1/2}$, w_0 the initial kinetic energy of the particle. Furthermore, the first invariant of the mirroring particle leads

$$\sin\alpha_E=\frac{(1+3\cos^2\theta_m)^{1/4}}{\sin^3\theta_m}. \tag{16}$$

Hereafter we use the non-dimensional variables defined by $\tilde{u}=u/u_0$ and $\tilde{t}=t/T$, where T is the transit-time of the hydromagnetic pulse along the field line, $T=4\int ds/V_A(s)$. The non-dimensional bouncing period is defined by $\tilde{T}_b=u_0T_b/r_E$. In Fig. 1, we show variations of $\tilde{T}_b$ and θ_m for the equatorial pitch angle α_E.

Substituting (15) into (1), basic relations to determine the particle bouncing motion in the stationary dipole field are

$$d\tilde{u}/d\tilde{t}=-b\frac{\cos\theta}{\sin^8\theta}\left[2+\frac{\sin^2\theta}{1+3\cos^2\theta}\right], \tag{17}$$

and

$$\tilde{u}=-(\sin\theta/\tilde{T}_b)(1+3\cos^2\theta)^{1/2}d\theta/d\tilde{t}, \tag{18}$$

where $b=3\tilde{T}_b\sin^2\alpha_E/2$. Since the above equations does not explicitly include the particle energy, numerical intergration of the above simultaneous differential equation determine completely the particle motion, if r_E and α_E are specified. For what follows we take $r_E=5R_E$ (R_E is a radius of the earth). Numerical integrations with different methods, Milne and Runge-Kutta-Merson, were performed and their

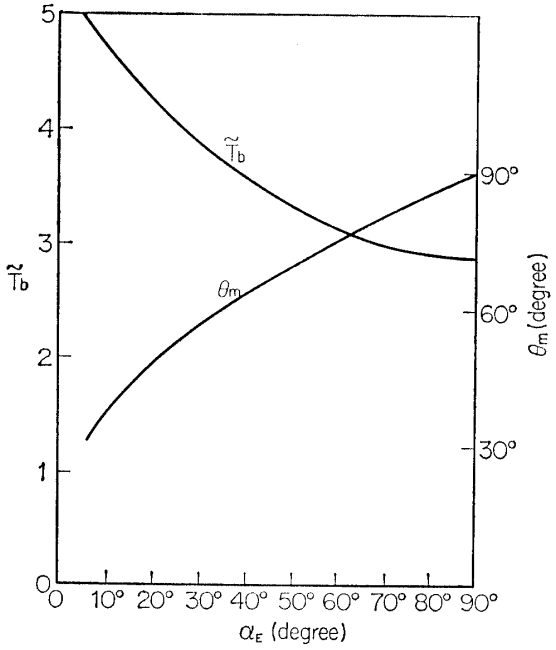

FIG. 1. Variations of colatitude of the mirror point, θ_m and non-dimensional bouncing period, $\tilde{T}_b$, for the trapped particles within the geomagnetic dipole field with equatorial pitch angle, α_E. The equatorial radial distance of the field line considered is 5 earth radii, $r_E=5R_E$.

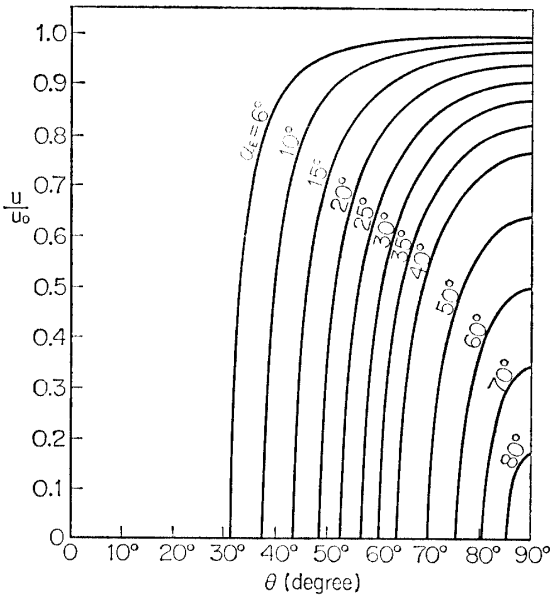

FIG. 2. Normalized particle velocities along the field line ($r_E=5R_E$) versus colatitude of the instantaneous particle position for various equatorial pitch angle.

results are shown in Fig. 2 for several equatorial pitch angles. Furthermore, the results also compared with ones obtained from the energy integral relation, $\tilde{u}=[1-(B_0(s)/B_E)\sin^2\alpha_E]^{1/2}$.

Distributions of ion concentrations and Alfvén speed

As a model of the thermal ion distribution, we consider that above the base of the magnetosphere (500 km altitudes) three kinds of ions, H^+, H_e^+, and O^+, are coexting under the diffusive equilibrium along a magnetic field line. With this assumption, distribution of the number density of each constituent can be determined by [*15*]

$$n_i(\theta)=n_{ib}[B_0(\theta)/B_b]^{1/2}\left\{\frac{\sum_j n_{jb}}{\sum_j n_{jb}\exp\left[-\frac{m_j g_0 R_E}{kT_e}\frac{R_E(r_E\sin^2\theta-R_E-Z_b)}{(R_E+Z_b)r_E\sin^2\theta}\right]}\right\}^{1/2}$$
$$\cdot\exp\left[-\frac{m_i g_0 R_E}{kT_e}\left(\frac{R_E}{R_E+Z_b}-\frac{R_E}{r_E\sin^2\theta}\right)\right] \tag{19}$$

where n_{jb}, T_e, and Z_b are the number density, temperature and altitudes of the base, g_0 is the surface gravity. Variations of ion concentrations along the field line of $r_E=5R_E$ are shown in Fig. 3. In this figure the relative variation of the

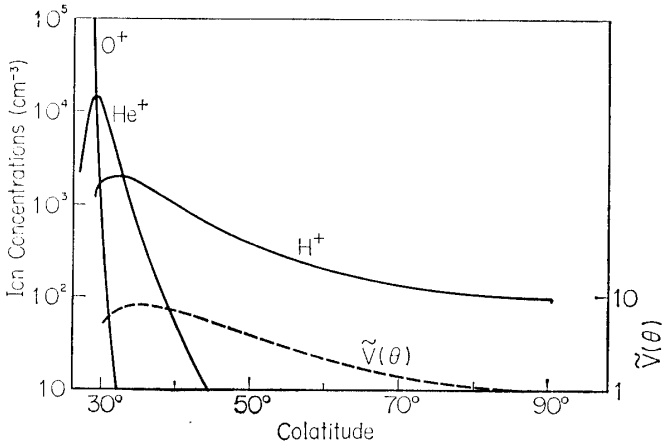

FIG. 3. Model distribution of the background plasma ion densities (full-lines) and the normalized Alfvén speed (broken line) along the field line ($r_E=5R_E$).

Alfvén speed resulting from these ion distributions, $\tilde{V}(\theta)=V_A(\theta)/V_{AE}$, where V_{AE} is the equatorial value of V_A, is also given.

5. Numerical Results *and* Discussion

Substitution of (4) and (15) into (1) leads to the following equation of motion as a basic equation

$$d\tilde{u}/d\tilde{t}=-(\mu B_E T/mr_E u_0)\{3(\cos\theta/\sin^8\theta)[2+\sin^2\theta(1+3\cos^2\theta)] \pm(\delta B_E/B_E)[\rho(\theta)/\rho_E]^{1/4}[2(a^2 r_E T/V_{AE})(\tilde{t}-|\tilde{\tau}|)/\tilde{V}(\theta) +|d\rho/\rho(\theta)d\theta|/4\sin\theta(1+3\sin^2\theta)^{1/2}]\cdot\exp[-a^2T^2(\tilde{t}-|\tilde{\tau}|)^2]\}, \quad (22)$$

where $\rho(\theta)=\sum_j m_j n_j(\theta)$ is density of the background plasma, and double signs $\pm$ are taken according to $\theta<\pi/2$ and $\theta>\pi/2$, respectively.

If the particle motion from the mirror point in high latitude to the equator on the northern hemisphere is considered, the first term on the right hand side of (22), which results from the dipole magnetic force, causes acceleration of a particle during the southward motion and decceleration during the northward motion. The second term, on the other hand, gives the net acceleration for the reflected particle due to the non-uniformly moving magnetic pulse. How much degree the particle can penetrate this magnetic wall region, and after then, the penetrating particle can be reflected by this barrier, depend on the initial situation before the effect of the head-on collision becomes appreciable. The third term resulting from the spatial variation of amplitude of the pulse yields the net decceleration.

At any rate, in order to have the particle reflection during the head-on collision with the magnetic pulse, the value of the right hand side of (22) becomes positive. From the preliminary consideration given in section 3, we see that the more flatterned the pitch angle of the penetrating particle is and the larger the amplitude of the pulse, $\delta B_E/B_E$, the more favourable the situation for the particle reflection

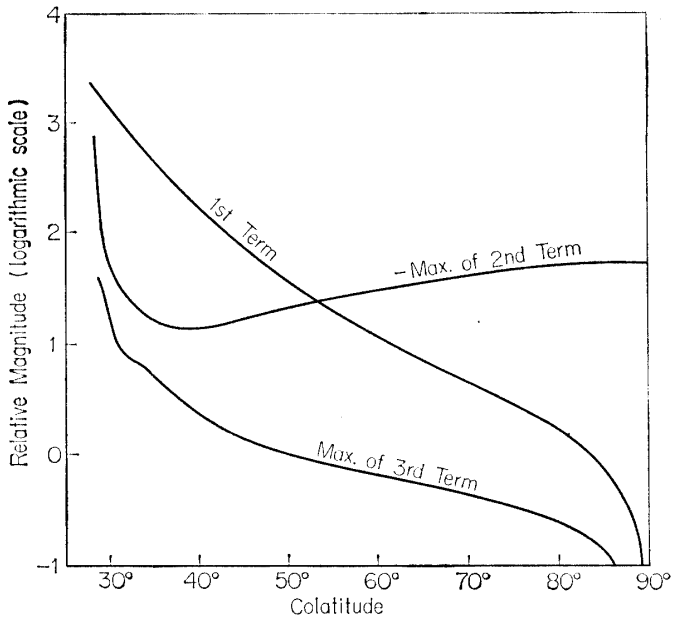

FIG. 4. Comparison of relative magnitudes of three forces for the particle motion [equation (22)]. First term corresponds to the dipole magnetic force, the second the magnetic force at the pulse front, and the third is due to the amplitude variation of the pulse.

becomes. For references, we plott the relative variation of three terms in a brace on the right hand side of (22) in Fig. 4, when $T=300$ sec, $aT=100$ and $\delta B_E/B_E=3$. From this figure, it would be suggested that a favourable condition for reflection by the magnetic pulse is only satisfied within the relatively low latitudes region. The effect of the amplitude variation of the pulse (the third term) may be unimportant.

The other equation to proceed the numerical integration is the definition of the local speed of a particle

$$\tilde{u}=-(r_E/u_0T)\sin\theta(1+3\cos^2\theta)^{1/2}d\theta/d\tilde{t}. \tag{23}$$

In the following, we consider an electron with $w_0=5$ KeV, and $u_0\gg\langle V_A\rangle$. If its equatorial pitch angle, α_E, initial position, s_0, and initial speed, $\tilde{u}_0$, which are previously given in the solution of the motion of trapped particles within the dipole field, are taken as initial conditions, numerical integrations of (22) and (23) determine the net acceleration and variation of the position of the mirror point of the particle under the complicated configuration considered here.

If Fig. 5, we show time-variations of the instantaneous position of the interacting particle (5 KeV electron) with various equatorial pitch angles, during the first two head-on collisions with the large-amplitude magnetic pulse of $\delta B_E/B_E=3$. In so far as the initial position of the particle is not close to the equatorial plane, an effect of θ_0 to the interaction is not important, since we have $u_0\gg V_A$. For the given parameters here, the critical equatorial pitch angle for the reflection by the magnetic pulse lies in somewhat between $\alpha_E=30°$ and $40°$. Particles with α_E being smaller

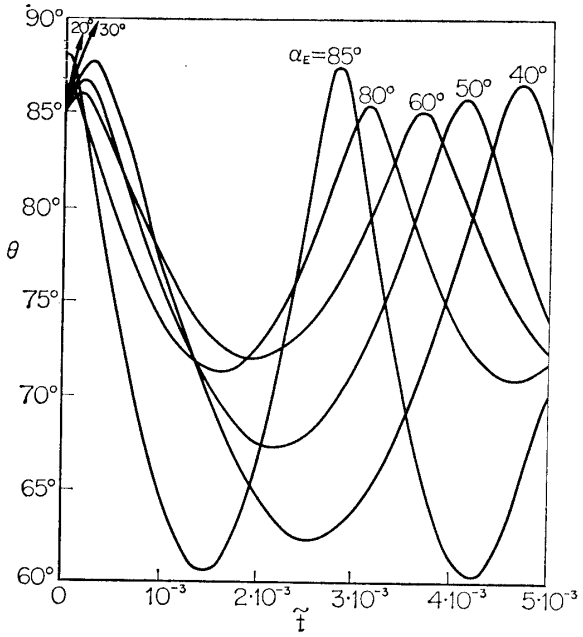

FIG. 5. Time variations of the instantaneous posision of an interacting particle during the begining few cycles of interaction. $\delta B_E/B_E=3$, $a=1/3$ and $T=300$ sec (see the text).

than this critical angle can completely penetrate the magnetic barrier, and then overtakes the other magnetic pulse on the southern hemisphere. Subsequent motion of these particles will be reconsidered elsewhere below.

Fig. 6 represents the effect of a difference of the effective thickness of the magnetic pulse for the particle motion. The upper part of this figure shows time-variations of the particle trajectory and the lower part the relative magnitude of the magnetic force within the barrier region of the pulse, for the two cases of $a=1$ and $1/3$. Since the magnetic force of the pulse is proportional to $(\tilde{t}-|\tilde{\tau}|)\exp[-a^2T^2(\tilde{t}-|\tilde{\tau}|)^2]$, there is a relatively large dimension of transition when a is small. Furthermore, the maximum magnetic force is inversely proportional to aT. Thus, for the case with smaller a, there is the larger retarding force for the penetrating particle and the effective interaction time is also longer. With this view, the result in Fig. 6 may be explained.

In Fig. 7 and 8, we show the full description of the interacting particle motion with $\alpha_E=70°$, during the first head-on collision, the subsequent multiple reflections, and after the moving magnetic mirror of the particle is finally over taken

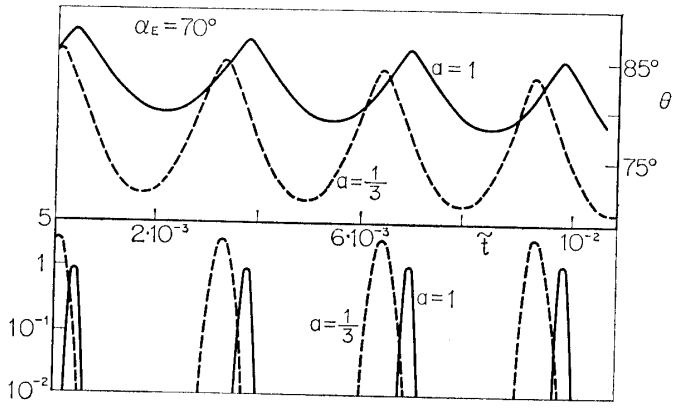

FIG. 6. Figures illustrating the effect of difference of the width of the pulse to the particle motion. The upper figure is time variations of the particle position and the lower the relative magnitude of the magnetic force within the pulse.

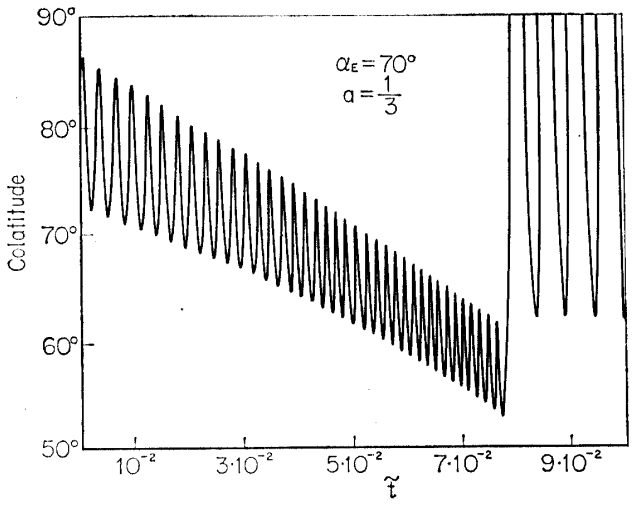

FIG. 7. The full illustration of the particle orbit during and after the interaction, (5 keV electrons and $\alpha_E=70°$).

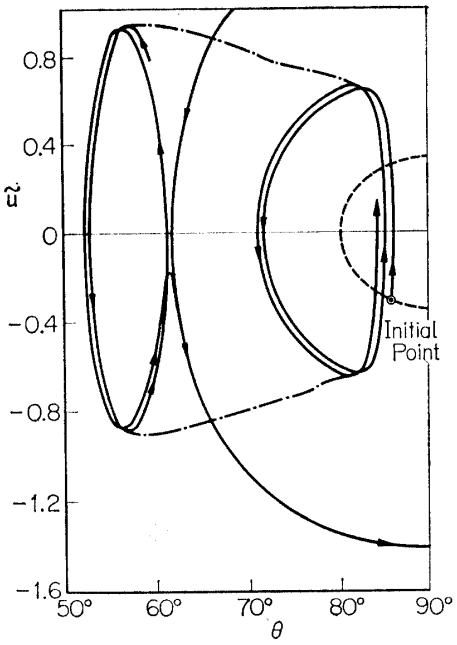

FIG. 8. Variation of the speed of 5 keV electron before, during and after the interaction. Dotted semicircle stands for the stationary bouncing motion, curves with arrows are the velocity orbit during the interaction, and dott-broken lines the envelopes of the latter. The largest curve with arrows corresponds to the accelerated bouncing motion.

TABLE 1. Variations of the mirror point and the maximum speed of the particle before and after the Fermi interaction.

equatorial pitch angle, α_E		30°	40°	55°	70°
colatitude of the mirror point,	before interactions, θ_m	56.9°	63.8°	72.6°	80.4°
	after interactions, θ_m*	58.3°	74.4°	63.2°	61.8°
the maximum speed,	before interactions, $\tilde{u}$	0.866	0.766	0.574	0.342
	after interactions, $\tilde{u}$*	0.780	0.472	1.156	1.420

by the magnetic pulse. The time-variation of the instantaneous position of the particle is given in Fig. 7, which shows the large change of the mirror point during the first interaction and subsequent secular slow change until the overtaking of the pulse occurs. Corresponding to this secular lowering of the mirror point, we have the slow acceleration as is seen in Fig. 8. The maximum acceleration after the interaction is of about 4 times and the mirror point varies from about 80° to 62°. In Table 1, we summarize the mirror point colatitude and the maximum speed of the particle at the equator before and after the multiple head-on collisions. From this, we see that the particle with the more flattened equatorial pitch angle receives

the more net acceleration and lowering of the mirror point. The particle with small pitch angle, on the contrary, suffers the net decceleration.

Summarizing, the Fermi acceleration due to multiple reflections of the particle with the moving magnetic pulse is most effective for trapped particles near the equator. However, since in the present calculation we assume the possible largest amplitude of the pulse, $\delta B_E/B_E=3$, which corresponds to the one-dimensional strong hydromagnetic compression (compression ratio=3), the above numerical

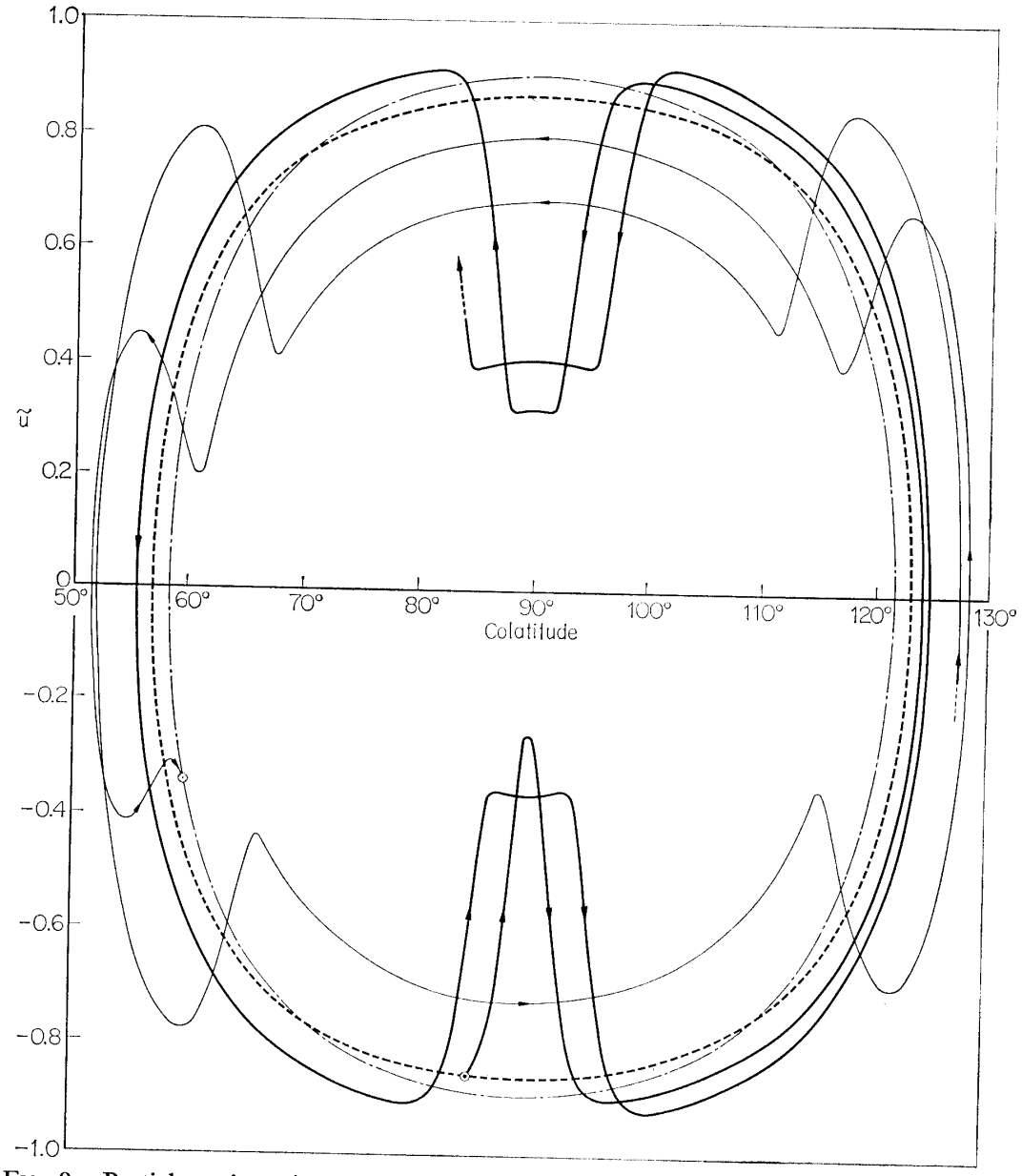

FIG. 9. Particle trajectories on the $\tilde{u}-\theta$ surface for the multiple bouncing electron with $\alpha_E=30°$, $w_0=5$ keV. The thick dotted curve represents the stationary trajectory in the dipole field before the interaction. The thin, full-broken curve is the stationary trajectory after multiple interactions of the electron with the moving pulses. Trajectories during few transite cycles just after the first interaction and just before last interaction are drawn by thick and thin full lines, respectively. The small circles with a dot and cross are the starting and end points of the interaction.

illustrations lead the negative conclusion for a possibility of the particle precipitation by such Fermi acceleration alone.

Next, if we consider the particle which can completely penetrate the moving barrier of the pulse at the first head-on collision, how is the motion of this particle modified during the subsequent multiple transites. In this case, the overtaking and head-on interaction of the particle with the pulse occur as a pair during small time interval. Consequently, the resulting net effect and its secular accumulation would not be appreciable. In Fig. 9, we give an illustration for this case.

In connection with the quasi-periodic precipitation of electrons with the period of several hundreds seconds at the ssc [*1, 10, 11*], we have the following question. Do geomagnetic pc 5 pulsations accompanying with ssc contribute to this energetic electron precipitation? More explicitly speaking, if we consider the standing hydromagnetic oscillations along the particular field line, can the secular accumulation of multiple transit-time acceleration of electrons during the increasing phase of amplitude of oscillations cause the appreciable precipitation of trapped electrons. Of course, if the period of oscillations is approximately the same order with the bouncing period of the interacting particle, this bounce-resonance interaction will yield appreciable effect. In the present case, however, $T_b \lesssim 1$ sec and $T \sim 300$ sec, we have only expect the secular accumulation of difference among consequent bouncings. In order to clear this possibility, it is necessary to solve the particle motion numerically, when the standing hydromagnetic oscillations of the even mode, for example $\delta B(\theta) = \delta B_E [\rho(\theta)/\rho_E]^{1/4} \cos 2\theta \sin \omega t$, is superposed on the dipole magnetic field.

Another possibility of particle acceleration associated with ssc is the direct acceleration by the electric field along the field lines within the localized region. Since the plasma compression within the magnetosphere at the time of ssc is not azimuthaly symmetric, the azimuthal drift motion of electrons and ions near the wave front will cause the space charge accumulations in opposite charges within two boader regions. These locally accumulated charges will be discharged along the field line during the transient stage of ssc. The intensity of the associated parallel electric field will considerably be different compared with that given in (2) for the simple sinusoidal oscillations. A stochastic acceleration due to the microscopic electrostatic waves with high-frequency, which may be excited by some instability mechanism associated with the large-scale adiabatic compression, has been remained as an unsolved possibility.

Ackowledgement

The present numerical analysis was made by the electric computor, HITAC-5020F, of the Computor Center, ISAS, University of Tokyo.

Department of Space Science
Institute of Space and Aeronautical Science
University of Tokyo, Tokyo
December 24, 1968

References

[1] K. A. Anderson: in *Earth's Particles and Fields*, Ed. by B. M. McCormac, Reinhold Book Corp., New York, (1968), p. 429, Also, R. R. Brown: Space Sci. Rev., **5**, 311, (1966).
[2] E. Schatzman: in *High Energy Astrophysics*, Ed. by C. Dewitt, E. Schatzman and P. Véron, Gordon and Breach, Sci. Pub., New York, Vol. II, (1967), p. 229.
[3] For examples, W. E. Drummond and D. Pines: Ann. of Phys., **28**, 478 (1964), and B. A. Tverskoi: Soviet Phys.-JETP, **26**, 821 (1968).
[4] C. F. Kennel and H. E. Petschek: J. Geophys. Res., **71**, 1 (1966).
[5] C. S. Roberts: in *Earth's Particles and Fields*, Ed. by B. M. McCormac, Reinhold Book Corp., New York, (1968), p. 317.
[6] I. B. McDiarmid and E. E. Budzinski: Can. J. Phys., **46**, 911 (1968).
[7] L. P. Block: Space Sci. Rev., **7**, 198 (1967).
[8] N. A. Krall: Phys. Fluids, **10**, 2263 (1967).
[9] M. N. Rosenbluth: in *Plasma Physics*, IAEA, Vienna, (1965), p. 485.
[10] T. Sato: Rep. Ionosp. Space Res. Japan, **16**, 295 (1962).
[11] K. A. Anderson: in *Aurora and Airglow*, Ed. by B. M. McCormac, Reinhold Pub. Corp., New York, (1967), p. 249.
[12] E. N. Parker: J. Geophys. Res., **66**, 693 (1961).
[13] A. Barnes: Phys. Fluids, **10**, 2427 (1967).
[14] T. Tamao: ISAS Rep., No. 422, (1968) and also Phys. Fluids, **12** (1969), in Press.
[15] T. Tamao: Sci. Rep. Tohoku Univ., Series 5, Geophysics, **17**, 43 (1965).